Available online at www.sciencedirect.com
SCIENCE DIRECT®
Trans. Nonferrous Met. Soc. China 18(2008) 541−547
Transactions of Nonferrous Metals Society of China
www.csu.edu.cn/ysxb/

Effect of processing way and aging treatment on properties and microstructures of 7B04 aluminum alloy

LI Nian-kui(李念奎)[1], LÜ Xin-yu(吕新宇)[2], CUI Jian-zhong(崔建忠)[1]

1. Key Laboratory of Electromagnetic Processing of Materials, Ministry of Education, Northeastern University, Shenyang 110004, China;
2. Northeastern Light Alloy Co. Ltd, Harbin 150060, China

Received 22 October 2007; accepted 14 December 2007

Abstract: The influence of forging and aging treatment on mechanical properties and microstructure of large size prestretched thick plate of 7B04 aluminium alloy was investigated through tensile test, corrosion test, transmission electronic microcopy(TEM) and energy dispersive spectrum(EDS) analysis. The results show that the properties of plate performed extra forging (FSR technology) are much higher than those of plate without forging (CSR technology). T7451 temper is preferred to resisting corrosion than T651 temper due to a wide PFZ and discontinuous grain boundary precipitates.

Key words: 7B04 aluminum alloy; processing way; aging; microstructure; exfoliation corrosion; stress corrosion

1 Introduction

The aerospace industry is constantly striving for improved materials that enable better performance at a reduced cost. With the development of high speed milling machines and the improved properties of thick plates, large structures machined from a thick plate can now replace forged components or built-up structures, which can significantly reduce the cost by minimizing the amount of components and joints. In recent years, 7xxx series (Al-Zn-Mg-Cu) aluminum alloy thick plates were used extensively in the aerospace field[1-6]. Two kinds of processing way were developed to produce the large size prestretched plate in thickness of 40−60 mm. One is that a flat ingot with a thickness of 400 mm is hot rolled through a special way to increase roll gap after homogenization annealing, and then undergoes consequent heat treatments (solid solution treatment→quench→stretch→ageing) to final products, which is called CSR for short. The other is that a plate with a thickness of 320 mm forged from a cylindrical ingot is hot rolled after homogenization annealing, and then undergoes the same consequent heat treatments to final products, which is called FSR for short. The FSR technology is firstly used in China. In present work, the tensile properties, corrosive properties and microstructures of this large size prestrethed thick plate processed by CSR and FSR technologies, respectively, are studied, in order to establish a proper way to produce the large size prestretched thick plate in batch.

2 Experimental

The 7B04 alloys were prepared using high pure aluminum, pure Zn, pure copper, pure Mg as well as master alloys of Al-Cu, Al-Mn and Al-Cr. The dimensions of flat ingot for CSR technology and cylindrical ingot for FSR technology are 440 mm×1500 mm×1200 mm and *d* 720 mm×2800 mm, respectively. The chemical compositions of ingots for the two technologies are listed in Table 1.

Table 1 Chemical compositions of 7B04 alloy for CSR and FSR technologies (mass fraction, %)

Ingot	Si	Fe	Cu	Mn	Mg
CSR	<0.1	0.21	1.54	0.31	2.65
FSR	0.08	0.21	1.53	0.31	2.50
Ingot	Cr	Ni	Zn	Ti	Al
CSR	0.13	<0.10	5.72	<0.05	Bal.
FSR	0.12	<0.10	5.55	<0.05	Bal.

Foundation item: Project(2003AA331100) supported by Commission of Science Technology and Industry for National Defence
Corresponding author: LI Nian-kui, Tel: +86-451-86564481; E-mail: linklnk@126.com

After homogenization annealing at 450−460 ℃ for 50 h, the CSR ingots were scalped and sawed to a slab with size of 400 mm×1 280 mm×1 200 mm and then hot rolled into plates with the thickness of 55 mm and 60 mm directly. While, the FSR ingots were scalped, sawed and forged into the slabs with size of 320 mm×1 280 mm×1 200 mm and then hot rolled into plates with the same size as CSR plates. Subsequently, all these plates underwent solid solution treatment, stretching and aging treatment. The solid solution treatment were carried out in a salt-bath at 470 ℃ for 80 min. Two kinds of aging treatment were applied in this work, T651 temper (120 ℃, 24 h) and T7451 temper (120 ℃, 8 h + 160 ℃, 18 h).

Tensile tests were carried out on a universal material testing machine WDW-100A in air at room temperature. The tensile velocity was 1 mm/min before yield and 15 mm/min after yield. The specimens for exfoliation corrosion test were immerged in a de-ionized or distilled aqueous solution of 234 g/L NaCl+50 g/L KNO_3+6.5 mL HNO_3 for 48 h at room temperature. The specimens for intergranular corrosion test were kept in a solution of 57 g/L NaCL+10 mL H_2O_2 for 24 h at room temperature. Tensile stress corrosion tests were done on a FY-06A machine in a solution of 3% NaCl+0.5% H_2O_2 at 35 ℃ with a temperature variation of ±1 ℃. Optical microstructures were observed on a Neophot-2 microscope after the specimens were etched by a solution of 5 mL HNO_3+5 mL HCL+10 mL HF+380 mL H_2O. The TEM observation was carried out on a transmission electron microscope TEM CM-12 with an accelerated voltage of 200 kV. Thin foils were prepared by twin-jet thinning electrolytically in a solution of 30% nitric acid and 70% methanol cooled by liquid nitrogen at 12 V, 100 mA. The EDX analysis was performed on a EDAX9100 machine. The conductivity of specimen was tested on a 7501 conductivity apparatus. Internal stress was measured on a XYL-73 machine, using a method of 0−45˚ to calculate the stress value.

3 Results

3.1 Microstructures and properties of CSR and FCR slabs

The tensile properties at room temperature and conductivity of CSR and FRS slabs are listed in Table 2. It can be seen that the tensile strength, elongation and conductivity of FSR slabs are higher than those of CSR slabs. The microstructures of the slabs after homogenization treatment are illustrated in Fig.1. For CSR slab (Fig.1(a)), some large eutectics and insoluble phases are located at grain boundaries, and plenty of fine dispersoids homogeneously distribute inside the grain. The microstructure of FSR slab is similar to that of CSR slab. However, some grains are still deformed and crushed. Eutectics and insoluble phases at grain boundaries become discontinuous and smaller.

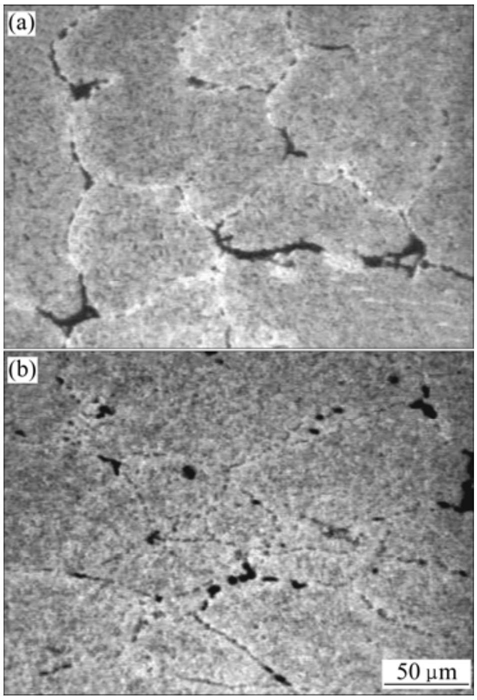

Fig.1 Optical microstructures of slabs after homogenization treatment: (a) CSR; (b) FCR

Table 2 Tensile properties at room temperature and conductivity of CSR and FRS slabs

Slab	σ_b/MPa	$\sigma_{0.2}$/MPa	δ/%	Conductivity/ $(MS\cdot m^{-1})$
CSR	193	82	5.0	22.6
FSR	226	104	13.7	24.7

3.2 Microstructures and properties of hot rolled thick plate for CSR and FCR

The tensile properties of hot rolled thick plate along transverse direction are listed in Table 3. The yield strength and elongation of hot rolled plate for FCR are higher than those of plate for CSR, but the ultimate tensile strength has no difference. The microstructures of hot rolled thick plates for CSR and FCR are presented in Fig.2. The remained phases are found to distribute along rolled direction for CSR plate (Fig.2(a)), while, become less and smaller for FCR plate, and the trend to distribute along rolled direction becomes unobvious (Fig.2(b)).

Table 3 Tensile properties of hot rolled thick plates for CSR and FCR at room temperature

Slab	σ_b/MPa	$\sigma_{0.2}$/MPa	δ/%
CSR	247	112	14.2
FSR	241	132	18.2

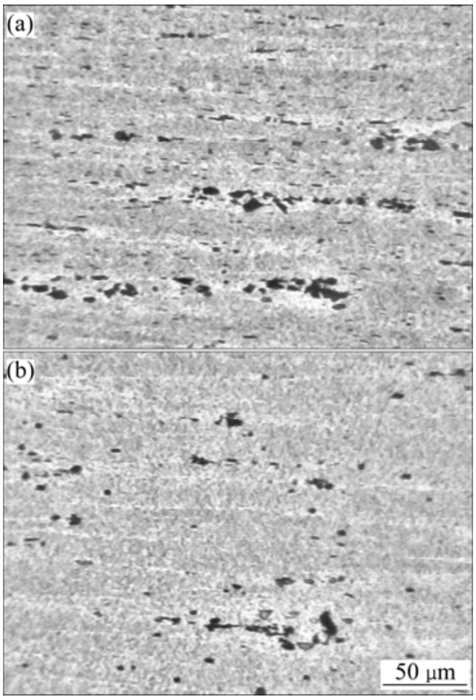

Fig.2 Optical microstructures of hot rolled thick plates on transverse section: (a) CSR; (b) FCR

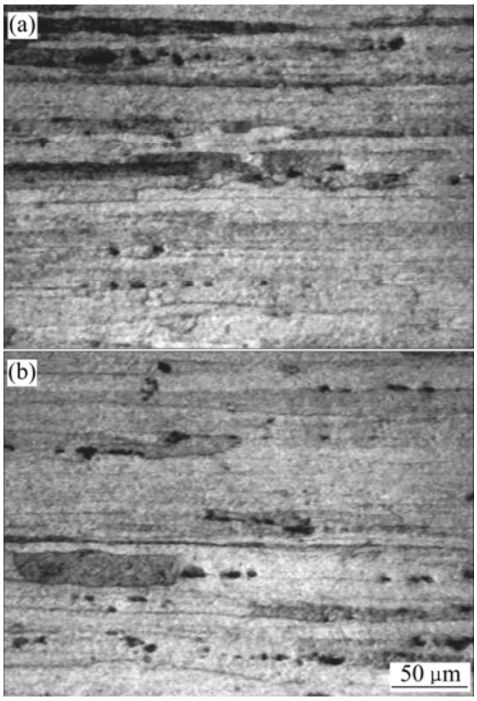

Fig.3 Optical microstructures of prestretched thick plates on transverse section after quench: (a) CSR; (b) FCR

3.3 Microstructures and properties of prestretched thick plate for CSR and FCR after quench

The tensile properties, conductivity and internal stress of the two kinds of prestretched thick plate after quench are listed in Table 4. It can be seen that the properties of the plates have no much difference in the state of pre-tensile, and there still have small amount of residual stress. The microstructures of the two kinds of plates are also presented in Fig.3. The amount and the size of the remained phases decrease further, and the recrystallized grains extended along rolling direction are found in both plates. The grain size is smaller and the grain boundary is more bending in FSR plate.

3.4 Microstructures and properties of CSR and FSR plates in T651 temper

The results of tensile properties, conductivity, residual stress and intergranular corrosion, exfoliation corrosion and tensile stress corrosion behaviors of CSR and FSR plates in T651 temper are listed in Table 5. The tensile strengths of CSR plate in transverse direction are higher than those of FSR plate, but the conductivity and residual stress are similar. Both CSR and FSR plates exhibit exfoliation corrosion. The CSR plate shows severe intergranular corrosion, while the FSR plate seems immune to it. The ability of resisting tensile stress corrosion of FSR plate is better than that of CSR plate.

Table 4 Properties of plates after quenching and stretching treatment

Slab	σ_b/MPa	$\sigma_{0.2}$/MPa	δ/%	Conductivity/(MS·m^{-1})	Internal stress/MPa		
CSR	421	379	12.4	15.8	−5.78	0	−8.53
FSR	433	379	15.3	16.2	−7.35	−0.78	−5.39

Table 5 Properties of CSR and FSR plates in T651 temper

Slab	Thickness/mm	Direction	σ_b/MPa	$\sigma_{0.2}$/MPa	δ/%	Conductivity/(MS·m^{-1})	Internal stress/MPa			Corrosive degree		
										Exfoliation	Intergranular	Tensile stress/h
CSR	55	T-L	582	555	6.67	18.34	−3.92	−2.94	−5.59	E_B	2	105, break
		S-T	508	−	3.33							
FSR	55	T-L	539	476	10.4	18.18	−4.21	−0.98	−3.12	E_B	No	720, not break
		S-T	504	−	2.0							

The 3D microstructures of CSR and FSR plates in T651 temper are illustrated in Fig.4. It can be seen that the recrystallized structures are observed in three directions, the grain elongated along the rolling direction and some second phases are also detected. Fine fiber structure is visible in T-L section.

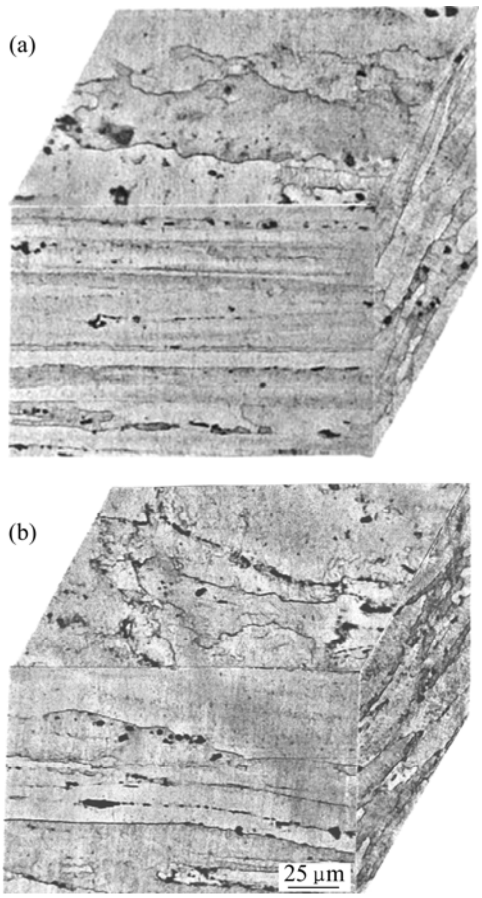

Fig.4 3D optical microstructures of plates in T651 temper: (a) CSR; (b) FSR

The TEM micrographs of CSR and FSR plates in T651 temper are shown in Fig.5. The intracrystalline precipitates of CSR plate are finer than those of FSR plate. The grain boundary precipitates of CSR plate exhibit in a continuous chain. The precipitate free zone (PFZ) of CSR plate is thinner than that of FSR plate. Some dark particles of about 100 nm are also found in the microstructures of the two kinds of plate. The EDX analysis indicates that some phases contain Al, Fe, Mn and Cu, and other phases bear Si and Cr which can not dissolve during subsequent homogenization treatment, hot rolling and solid solution treatment.

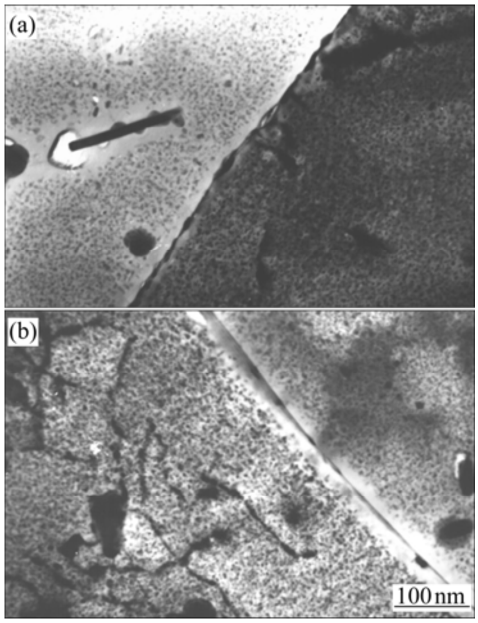

Fig.5 TEM micrographs of plates in T651 temper: (a) CSR plate; (b) FSR plate

3.5 Microstructures and properties of CSR and FSR plates in T7451 temper

The results of tensile properties, conductivity, residual stress and intergranular corrosion, exfoliation corrosion and tensile stress corrosion behaviors of CSR and FSR plates in T7451 temper are listed in Table 6. It can be seen that, except residual stress, the other mechanical properties of the two kinds of plates in T7451 temper are higher than those of plates in T651 temper. The tensile properties of FSR plate are a little bit higher than those of CSR plate. No intergranular corrosion is found in CSR and FSR plates. The resistance of stress corrosion and exfoliation corrosion of FSR plate are better than those of CSR plate.

The 3D microstructures of CSR and FSR plates in T7451 temper are demonstrated in Fig.6. The totally recrystallized grains are observed in three directions, but the elongated grain along the rolling direction and some

Table 6 Mechanical Properties of CSR and FSR plates in T7451 temper

Slab	Thickness/mm	Direction	σ_b/MPa	$\sigma_{0.2}$/MPa	δ/%	Conductivity/($MS\cdot m^{-1}$)	Internal stress/MPa			Corrosive degree		
										Exfoliation	Intergranular	Tensile-stress/h
CSR	60	T-L	512	432	10.7	21.62	2.35	0.88	4.60	E_A	No	723, break
		S-T	454	−	4.67							
FSR	60	T-L	532	463	11.3	21.71	−0.98	−2.45	2.45	E_P	No	744, not break
		S-T	427	−	2.66							

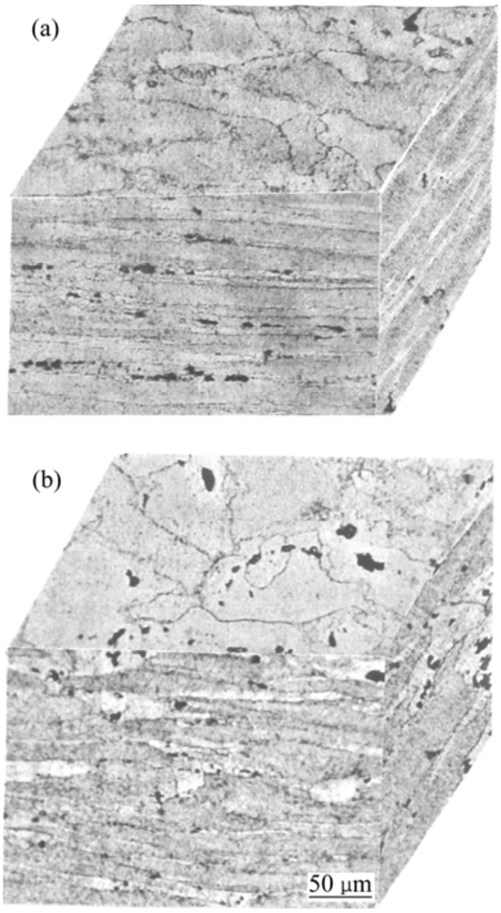

Fig.6 3D optical microstructures of plates in T7451 temper: (a) CSR; (b) FSR

second phases are found. Fine fiber structure is detected in T-L section of CSR plate, but some recrystallized grains are discovered besides fiber structure in FSR plate.

The TEM micrographs of CSR and FSR plates in T7451 temper are shown in Fig.7. The intracrystalline precipitates in both CSR and FSR plates are coarser and the PFZs are wider than those in T651 temper. The intracrystalline precipitates in FSR plates are bigger and PFZs are wider than those in CSR plates. The EDX analysis indicates that the second phase contains Al, Fe, Mn and Cu.

4 Discussion

Because the FSR slab is forged after DC casting, many dislocations and substructures are detected in the matrix, the size of second phase is fine, and the strength and plasticity are higher than those of CSR slab. This kind of structure still remains during hot rolling and pre-tensile test, so the plasticity of FSR plate in T651and T7451 is higher than that of CSR plate. But the strength of FSR plates and CSR plates is quite same due to the similar microstructures.

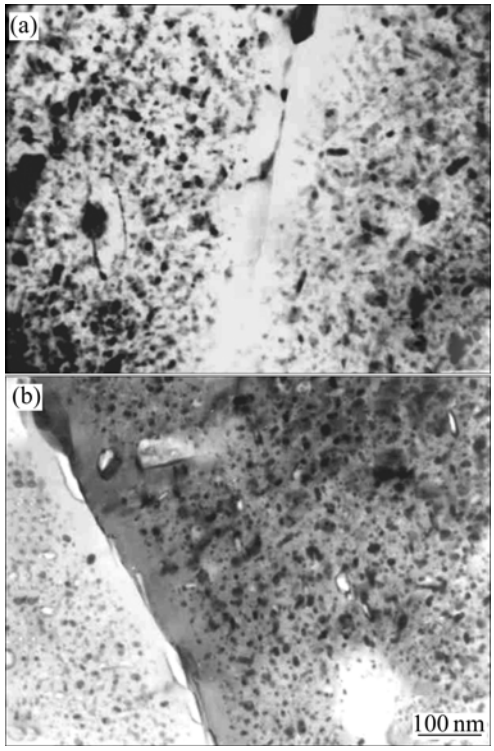

Fig.7 TEM micrographs of plates in T7451 temper: (a) CSR; (b) FSR

The generally accepted precipitation sequences for 7000 series alloys are as follows[7−10]: supersaturated solid solution(SSS)→coherent stable GP zones→semi-coherent intermediate $\eta'(MgZn_2)$ → incoherent stable $\eta(MgZn_2)$ or T(AlZnMgCu). The morphology size and the degree of coherent with the matrix will influence the properties of aluminium alloy. The contribution of semi-coherent intermediate $\eta'(MgZn_2)$ to the strength is greater than that of GP zones. The incoherent stable $\eta(MgZn_2)$ contributes less than GP zones and η'. In T651 temper, the microstructure of CSR plate has fine and homogeneously distributed matrix precipitates, continuous grain boundary precipitates and very thin PFZ, and the matrix precipitates are mainly GP zone and a few of η' phase[11]. The FSR plate undergoes extra hot working compared to CSR plate, the eutectics dissolve completely during processing, and the degree of solute saturation is higher after quenching. Under similar aging condition of CSR and FSR plate, GP zone will grow to η', so the matrix precipitates are coarser than those of CSR plate. But the size of η' phase is still small. The dislocations can pass it by cutting, and the subsequent deforming will proceed along this preferring site, so the strength is low. Additionally, PFZ is wider and the matrix precipitates are larger in FSR plate, which indicates the alloy has been overaged, so the strength is lower than that of CSR plate. In T7451 temper, the main matrix precipitates are η' in CSR and FSR plates, and the precipitation density is very low. Furthermore, the grain boundary precipitates, recognized as the η phase[11], grow up to be coarser and are more sparsely distributed, and the PFZ of 30−40 nm in width can also be observed. All these phenomena contribute to the characteristics of over aging. So it is not surprising that the alloy possesses low tensile strength under this aging temper.

After quenching, high internal stress generates in the thick plate. Part of the internal stress can be removed by the process of straightening and pre-tensile, but the stress produced by dislocation and the distortion of lattice can not be eliminated. The residual stress in the plate after quenching and pre-tensile are still great as listed in Table 4. During one-step aging treatment, the remained dislocations and the proliferated dislocations by pre-tensile will move and react, the positive and negative dislocations will counteract, and most distortion of lattice will be eliminated, so the internal stress decreases. The results also indicate that the internal stress in the thick plate in T651 temper is lower than that in pre-tensile state. The two-step aging treatment decreases the internal stress further.

Exfoliation corrosion nucleates and propagates along the grain boundaries. The grain orientation and the type of grain boundary precipitates significantly influence the corrosion behavior of alloy. The microstructure of CSR plate has strong preferring orientation after quench and aging, but this trend in FSR plates is weak. Corrosion in CSR plates propagates quickly along the elongated boundaries parallel to transverse section, so exfoliation corrosion is severe. The grain boundary precipitates in CSR plates are fine and continuous compared to those in FSR plate, which is in favor of forming preferring corrosion channel[12] and promotes exfoliation corrosion and intergranular corrosion.

The stress corrosion failure of Al-Zn-Mg-Cu alloy is one of the important factors limiting its applications. Some researchers considered that the SCC in 7xxx alloy is caused by hydrogen brittleness[12−18]. So far, the “Mg-H” mechanism is the principal theory for hydrogen brittleness of 7xxx alloy. The process of stress corrosion is the hydrogen fracture[13]. The alloy surface and environment water will have several electrochemical reaction when the alloy endures the pull stress:

$$2Al+3H_2O \rightarrow Al_2O_3+6H^++6e^-$$

$$Al \rightarrow Al^{3+}+3e^-$$

$$H^++e^- \rightarrow [H]$$

Traveled by absorption, diffusion and dislocation, the atomic hydrogen will gather around the grain boundary precipitates (η), and accelerates the crack propagation along grain boundary. At the same time, Cl ion will assist the destroy of the passivating film at the junction of grain boundary and surface under stress, and then anode dissolution will happen along grain boundary. The segregation of Mg at the grain boundary increases the hydrogen brittleness. Mg is easy to form “Mg-H” composite, which will accelerate the absorption of H, and increase the solid solubility of H at grain boundary. KANNO et al[18] thought that the amount of η and η' increased with the prolonging of aging treatment, and the content of Mg at grain boundary decreased, so the probability of hydrogen brittleness reduced. It is the reason that the SCC resistance under overageing enhances.

Aging treatment influences the stress corrosion sensitivity significantly. Under-aging is the highest, peak-aging is middle and over-aging is the lowest[13]. In T651 temper, the over-aging microstructure in FSR plate is preferred to resisting stress corrosion than the peak-aging microstructure in CSR plate. In T7451 temper, the wide PFZ and discontinuous grain boundary precipitates make the alloy a better ability of resisting stress corrosion than in T651 temper.

Stress corrosion always happens at grain boundary. Aging treatment will change the structure of intragrain and grain boundary. The continuously distributed precipitates at grain boundary in peak-aging temper will become the crack propagation channel under corrosive solution attack. Under two-step aging, with the growth of precipitates, the distance between precipitates increases, so the corrosive channel becomes discontinuous. The appearance of more stable phases will change the electrochemical property at grain boundary[15], so improve the stress corrosion resistance.

5 Conclusions

1) Completely recrystallized microstructure after quenching and aging are detected in CSR and FSR plates. The grains and second phase in CSR plate are strongly preferred orientation than those in FSR plate.

2) In T651 temper, the strength of FSR plate is lower and the plasticity is higher than those of CSR plate.

3) In T7451 temper, the properties of FSR plates are higher than those of CSR plates.

4) T7451 temper is in favor of stress elimination.

References

[1] HEINZ A, HASZLER A, KEIDEL C, MOLDENHAUER S, BENEDICTUS R, MILLER W S. Recent development in aluminium alloys for aerospace applications [J]. Materials Science and Engineering A, 2000, 280(1): 102−107.

[2] MOLDENHAUER S, VAN DER LUGT J, HOOGLAND H, BENEDICTUS R, MILLER W S, HEINZ A, KEIDEL C, HASZLER A. Recent improvement in high strength thick AA7050-plate [J]. Materials Science Forum, 2000, 331: 1101−1106.

[3] KE Y L, DONG H Y. Pre-stretching process and its application in reducing residual stress of quenched 7075 aluminum alloy thick-plates [J]. The Chinese Journal of Nonferrous Metals, 2004, 14(4): 639−645. (in Chinese)

[4] DUMONT D, DESCHAMPS A, BRECHET Y. On the relationship between microstructure, strength and toughness in AA7050 aluminum alloy [J]. Materials Science and Engineering A, 2003, 356(1/2): 326−336.

[5] LI Z H, XIONG B Q, ZHANG Y A, ZHU B H, LIU H W, WANG F. Effect of one-step ageing on microstructure and properties of 7B04 pre-stretched thick plate [J]. The Chinese Journal of Nonferrous Metals, 2005, 15(11): 1670−1674. (in Chinese).

[6] MILLER M P, HARLEY E J, TURNER T J, BEAUDOIN A J, CASSADA W A. Mechanical behavior of thin sheets machined from AA7050-T7451 plate [J]. Materials Science Forum, 2000, 331: 1243−1248.

[7] DANH D. A TEM study of microstructural changes during retrogression and reageing in 7075 aluminum [J]. Metallurgical Transactions A, 1983, 14(9): 1843−1850.

[8] PARK J K, ARDELL A J. Microstructures of the commercial 7075Al alloy in the T651 and T7 tempers [J]. Metallurgical Transactions A, 1983, 14(10): 1957−1965.

[9] BERG L K, GJONNE J, HANSEN V, LI X Z, KNUTSON-WEDEL M, WATERLOO G, SCHRYVERS D, WALLENBERG L R. GP-zones in Al-Zn-Mg alloys and their role in artificial aging [J]. Acta Materialia, 2001, 49: 3443−3451.

[10] SHA G, CEREZO A. Early-stage precipitation in Al-Zn-Mg-Cu alloys (7050) [J]. Acta Materialia, 2004, 52: 4503−4516.

[11] TADAKAZU O, HIDEAKI S. Heat treatment to reduce the susceptibility of AL-Zn-Mg-Cu alloy to stress corrosion cracking [J]. Journal of Japan Institute of Light Metals, 1986, 36(10): 647−656.

[12] RAJAN K, WALLACE W, BEDDOES J C. Microstructural study of high-strength stress-corrosion resistant 7075 aluminium alloys [J]. Journal of Materials Science, 1982, 17(10): 2817−2824.

[13] SONG R G, DIETZEL W, ZHANG B J, LIU W J, TSENG M K, ATRENS A. Stress corrosion cracking and hydrogen embrittlement of an Al-Zn-Mg-Cu alloy [J]. Acta Materialia, 2004, 52: 4727−4743.

[14] SRIVASTAN T S. Microstructure, tensile properties and fracture behaviour of aluminium alloy 7175 [J]. Journal of Materials Science, 1992, 27(17): 4772−4781.

[15] ZIELINSKI A, RENAULD E, PUIGGALI M, OLIVE J M, CID M, DESJARDINS D. Effects of tempers on environmental-assisted failure of an Al-Zn-Mg-Cu alloy [J]. Journal of Materials Processing Technology, 1995, 53(1/2): 491−498.

[16] ROBINSON J S. Influence of retrogressing and reaging on the stress corrosion cracking resistance of 7010 [J]. Materials Science Forum, 2000, 331: 1653−1658.

[17] PUIGGALI M, ZIELINSKI A, OLIVE J M, RENAULD E, DESJARDINS D, CID M. Effect of microstructure on stress corrosion cracking of an Al-Zn-Mg-Cu alloy [J]. Corrosion Science, 1998, 40(4/5): 805−81.

[18] KANNO M, SAITOH H, SUZUKI H. Effect of copper on intergranular fracture of Al-Zn-Mg alloy [J]. Journal of Japan Institute of Light Metals, 1987, 37(5): 375−380.

(Edited by YUAN Sai-qian)